Research article

Journal of RAMAN SPECTROSCOPY

Received: 30 November 2013 Revised: 14 June 2014 Accepted: 17 June 2014 Published online in Wiley Online Library: 17 July 2014

(wileyonlinelibrary.com) DOI 10.1002/jrs.4548

Raman study of different crystalline forms of $PbCrO_4$ and $PbCr_{1-x}S_xO_4$ solid solutions for the noninvasive identification of chrome yellows in paintings: a focus on works by Vincent van Gogh†

Letizia Monico,[a,b] Koen Janssens,[b] Ella Hendriks,[c] Brunetto G. Brunetti[d,a] and Costanza Miliani[a,d]*

Chrome yellows, a class of pigments frequently used by painters of the Impressionism and Post-impressionism period, are known for their different chemical stability; the latter depends on the chemical composition ($PbCrO_4$, $PbCr_{1-x}S_xO_4$) and crystalline structure (monoclinic or orthorhombic) of the material. The possibility to distinguish among different forms of this pigment is therefore relevant in order to extend knowledge on the corresponding degradation process that is observed on several original paintings. For this purpose, three paintings conserved at the Van Gogh Museum (Amsterdam) were analyzed using noninvasive Raman spectroscopy, while equivalent investigations employing bench-top instrumentation were performed to obtain information from micro-samples originating from these works of art. In each painting, the chrome yellow was identified either as monoclinic $PbCrO_4$ or in the form of monoclinic $PbCr_{1-x}S_xO_4$ ($x < 0.25$) or S-rich orthorhombic $PbCr_{1-x}S_xO_4$ ($x \sim 0.5$). Our ability to make this fairly subtle distinction is based on a Raman study of several oil paint model samples made up of monoclinic and/or orthorhombic crystalline forms of $PbCrO_4$ and $PbCr_{1-x}S_xO_4$ ($0.1 \le x \le 0.8$). These paints were studied using several excitation wavelengths (namely 785.0, 532.0, 514.5, and 488 nm). Because of the absence of the resonance Raman effect, which strongly enhances the chromate symmetric stretching band, and the absence of any laser-induced photodecomposition, it is advantageous to acquire data at 785.0 nm. The band-shape and the position of the chromate bending modes proved to be more sensitive to the solid solution composition and crystalline structure than the stretching modes and can be used as distinctive spectral markers to discriminate among the different chrome yellow forms that are present.

Additional supporting information may be found in the online version of this article at the publisher's web site.

Keywords: chrome yellow; Van Gogh; noninvasive; coprecipitate; paintings

Introduction

Chrome yellow is a synthetic pigment that is encountered in paintings of the 19th–early 20th century, such as those by Turner (1775–1851),[1] Constable (1776–1837),[2] Pissarro (1830–1903),[3] Cézanne (1839–1906),[4] Monet (1840–1926),[5] Van Gogh (1853–1890),[6,7] Seurat (1859–1891),[8] and Ensor (1860–1949).[9] It has the chemical composition of pure lead chromate ($PbCrO_4$ found in nature as the mineral crocoite) or of solid solutions of lead chromate and lead sulfate ($PbCr_{1-x}S_xO_4$), with shades that range from yellow to orange ($x < 0.1$) and pale yellow ($x > 0.5$) with increasing sulfate concentration.[10,11] Depending on the sulfate amount, chrome yellow is nowadays named Primrose/pale Lemon Chrome ($PbCr_{1-x}S_xO_4$, $0.4 \le x \le 0.5$), Lemon Chrome ($PbCr_{1-x}S_xO_4$, $0.2 \le x \le 0.4$), and Middle Chrome (mainly $PbCrO_4$).[10,12] Three varieties of chrome yellow are mentioned in several of Van Gogh's letters of the period 1888–1890 as chrome yellow types 1, 2, and 3, possibly corresponding to the 'lemon', 'yellow' and 'orange' shades (see paint orders in letters 595, 684, 687, 710, and 863 and color annotated sketches F-/JH 1463 and F-/JH 1428 in letter 622, for example).[7]

The solid solution end members $PbCrO_4$ and $PbSO_4$ have monoclinic [$P2_{1/n}$ space group, (C_{2h}^5), $Z = 4$][13] and orthorhombic crystalline structures [P_{nma} space group, (D_{2h}^{16}), $Z = 4$],[14] respectively. As a consequence, when x increases beyond 0.4, a change from a monoclinic to an orthorhombic structure is observed in $PbCr_{1-x}S_xO_4$.[15]

* *Correspondence to: Costanza Miliani, Istituto CNR di Scienze e Tecnologie Molecolari (CNR-ISTM), c/o Dipartimento di Chimica, Università degli Studi di Perugia, via Elce di Sotto 8, I-06123 Perugia, Italy.*
E-mail: costanza.miliani@cnr.it

† *This article is part of the special issue of the Journal of Raman Spectroscopy entitled "Raman in Art and Archaeology 2013" edited by Polonca Ropret and Juan Manuel Madariaga.*

a *Istituto CNR di Scienze e Tecnologie Molecolari (CNR-ISTM), c/o Dipartimento di Chimica, Università degli Studi di Perugia, via Elce di Sotto 8, I-06123, Perugia, Italy*

b *University of Antwerp, Department of Chemistry, Groenenborgerlaan 171, B-2020, Antwerp, Belgium*

c *Van Gogh Museum, Paulus Potterstraat 7, 1070 AJ, Amsterdam, The Netherlands*

d *Centre SMAArt and Dipartimento di Chimica, Biologia e Biotecnologie, Università degli Studi di Perugia, via Elce di Sotto 8, I-06123, Perugia, Italy*

Artists, such as Van Gogh, were well aware that (see letters 538 and 595)[7] chrome yellows show a tendency to lose their original bright yellow color, thereby becoming greenish-brown when exposed to sunlight. Also, other types of environmental factors, such as contaminants and/or atmospheric gases (e.g., SO_2 and H_2S), can have this effect.[16–18] Considering that this phenomenon is thought to be one of the causes that has led to changes in the original color scheme of several paintings by Van Gogh and some of his contemporaries, the understanding of the alteration mechanism of chrome yellows is highly relevant in the field of paintings conservation.

Previous investigations by synchrotron radiation X-ray methods and energy electron loss spectroscopy carried out on photochemical aged model samples and on two paint micro-samples taken from paintings by Van Gogh allowed us to demonstrate that (i) the degradation mechanism involves a reduction of Cr(VI) to Cr (III) and (ii) the process is favored when the pigment is present in the orthorhombic S-rich $PbCr_{1-x}S_xO_4$ ($x > 0.4$) form.[19–22] In addition, X-ray diffraction (XRD), micro-Raman, and micro-FTIR analysis of paint cross-sections demonstrated that Van Gogh frequently made use of various forms of this pigment, including the more unstable ones.[23]

Indeed, the possibility to noninvasively assess the presence of different types of chrome yellow in painting collections becomes therefore relevant as part of their proper conservation and public display.

In this context, the present work is aimed at (i) extending our knowledge on the Raman scattering features of $PbCrO_4$ and $PbCr_{1-x}S_xO_4$ solid solutions and (ii) evaluating the possibility of distinguishing among different forms of the chrome yellow pigments in works of art by means of portable fiber optic Raman spectroscopy. For this purpose, a systematic Raman study of oil paint models made up of six lead chromate pigments [$PbCrO_4$ and $PbCr_{1-x}S_xO_4$ ($0.1 \le x \le 0.8$) monoclinic and/or orthorhombic] by means of bench-top and portable instrumentation is presented. The most appropriate experimental conditions (i.e. choice of the excitation wavelength and laser power) to effectively identify the types of lead chromate-based compounds and prevent any laser-induced damage of the painting are discussed.

The information acquired from the investigations of paint models is used to interpret the noninvasive Raman spectra recorded directly from the surface of three Van Gogh paintings conserved at the Van Gogh Museum in Amsterdam (*Sunflowers gone to seed*, *Bank of the Seine*, and *Portrait of Gauguin*).

Experimental

Materials

Synthesis of $PbCrO_4$ and $PbCr_{1-x}S_xO_4$ and preparation of paint model samples

Powders of monoclinic $PbCrO_4$ (sample S^*_{1mono}) and of four different coprecipitates of the form $PbCr_{1-x}S_xO_4$ [samples S^*_{3A} ($x \sim 0.1$), S^*_{3B} ($x \sim 0.25$), S^*_{3C} ($x \sim 0.5$), S^*_{3D} ($x \sim 0.75$)] and of orthorhombic $PbCrO_4$ (sample S^*_{1ortho}) were synthesized following the experimental procedures described in our previous works.[21,23] The asterisk is used to denote the dry pigment powders, i.e. prior to mixing with a binding medium.

Paint models denoted S_1–S_{3D} were obtained mixing these in-house synthesized powders with linseed oil in a 4 : 1 weight ratio and applying the mixtures on polycarbonate microscopy slides. Additional paint samples were prepared mixing S^*_{1mono} and either S^*_{3B} or S^*_{3D} in different weight ratio (1 : 9, 1 : 3, 1 : 1, 3 : 1, 9 : 1) with linseed oil.

A list of the in-house synthesized lead chromate-based compounds and some of their structural properties obtained *via* XRD investigations are reported in Table 1 (see also the work of Monico *et al.*[23] for further details). Powder XRD analysis revealed that samples S^*_{1mono}, S^*_{3A} and S^*_{3B} are almost entirely composed of a single monoclinic phase, while a progressive increase of the amount of the orthorhombic $PbCr_{0.1}S_{0.9}O_4$ phase and a decrease in abundance of the monoclinic $PbCr_{1-x}S_xO_4$ solid solution material can be observed when passing from S^*_3c to S^*_{3D}. In these two latter samples, minor amounts of orthorhombic $PbCrO_4$ were also identified. In agreement with an earlier study on $PbCr_{1-x}S_xO_4$ solid solutions,[15] the unit cell volume of the solid solutions decreases concomitantly with the increase of sulfate content (as an example Fig. S1 of Supporting Information shows the experimentally determined change of the unit cell volume for $S^*_{1mono} - S^*_{3D}$ monoclinic phase *versus* the sulfate concentration).

Original paintings and corresponding embedded paint micro-samples

Raman investigations were performed on the following Van Gogh paintings exhibited at the Van Gogh Museum in Amsterdam: *Sunflowers gone to seed*, *Bank of the Seine*, and *Portrait of Gauguin*.

Noninvasive Raman measurements on paintings were carried out during an European transnational access of the mobile laboratory.[24] Further details about the paintings and micro-samples investigated are summarized in Table 2. Figures S2–S4 (Supporting Information) show the sampling areas and a selection of some among the locations where noninvasive Raman analysis was performed.

Three corresponding paint micro-samples taken from each of the painting: *Sunflowers gone to seed* (sample F377/2), *Bank of the Seine* (sample F293/3), and *Portrait of Gauguin* (sample ×448/2) were previously studied by Raman and synchrotron XRD. Raman spectra are here discussed in detail and critically compared with the noninvasive data.

Methods

Bench-top micro-Raman

Analysis of both paint models and original paint micro-samples was performed by means of a JASCO NRS-3100 double-grating spectrophotometer connected to an optical microscope (100× objective) and equipped with a charge coupled device detector cooled up to −47 °C.

Paint models were subject to preliminary investigation using the following excitation wavelengths: 488.0 and 514.5 nm (Argon ion laser), 532.0 nm (Nd:YAG laser), and 785.0 nm (diode laser). For the spectra collected using 488.0, 514.5, and 532.0 nm excitation, the laser power at the sample was kept around 1 mW, and a 1200 lines/mm grating was employed. For the profiles recorded at 785.0 nm, power values between 3 and 7 mW and a 600 lines/mm grating were used. Spectra were recorded in the energy range of 2000–250 cm^{-1}; the exposure time varied between 3 and 10 s, with 3–10 accumulations. The spectral resolution was between 2 and 4 cm^{-1}. In the same experimental conditions, the diode laser was also used to record spectra from the paints prepared mixing different types of chrome yellow.

Table 1. Composition of in-house synthesized lead chromate-based powders and corresponding results of the Rietveld quantitative analysis of the XRD patterns (see the work of Monico *et al.*[23] for further details)

Sample[a]	Starting molar ratio CrO_4^{2-}:SO_4^{2-}	Rietveld quantitative analysis results						
		Phases present	Space group	Lattice parameters (Å)			Unit cell volume (Å^3)	Mass fraction (%)
				a	b	c		
S^*_{1mono}[b]	1 : 0	$PbCrO_4$	Monoclinic $P2_1/n$	7.12806(6)	7.43747(6)	6.80152(6)	360.581(5)	98.82(5)
		$PbCrO_4$	Orthorhombic *Pnma*	8.667(2)	5.548(1)	7.118(2)	342.3(1)	1.18(6)
S^*_{3A}	0.9 : 0.1	$PbCr_{0.89}S_{0.11}O_4$	Monoclinic $P2_1/n$	7.1189(1)	7.4268(1)	6.7907(1)	359.029(9)	100
S^*_{3B}	0.75 : 0.25	$PbCr_{0.76}S_{0.24}O_4$	Monoclinic $P2_1/n$	7.0928(2)	7.3956(2)	6.7709(2)	355.17(2)	100
S^*_{3C}[b]	0.5 : 0.5	$PbCr_{0.54}S_{0.46}O_4$	Monoclinic $P2_1/n$	7.0715(2)	7.3733(2)	6.7538(2)	352.15(2)	60.0(2)
		$PbCr_{0.09}S_{0.91}O_4$	Orthorhombic *Pnma*	8.5113(2)	5.4055(2)	6.9836(3)	321.30(2)	31.1(1)
		$PbCrO_4$	Orthorhombic *Pnma*	8.6457(9)	5.5780(5)	7.0881(6)	341.83(6)	9.10(8)
S^*_{3D}[b]	0.25 : 0.75	$PbCr_{0.6}S_{0.4}O_4$	Monoclinic $P2_1/n$	7.0743(5)	7.3779(6)	6.7634(6)	353.01(5)	11.5(3)
		$PbCr_{0.1}S_{0.9}O_4$	Orthorhombic *Pnma*	8.4994(2)	5.4035(1)	6.9736(1)	320.27(1)	74.7(3)
		$PbCrO_4$	Orthorhombic *Pnma*	8.612(1)	5.5881(9)	7.095(1)	341.44(8)	13.8(2)

[a]The Rietveld quantitative analysis was not performed to S^*_{1ortho}. Its XRD pattern shows features similar to that reported in the literature.[15] (see the work of Monico *et al.*[23] for details).

[b]The weighted average unit cell volume for S^*_{1mono}, S^*_{3C}, and S^*_{3D} was approximately estimated to be 360.36(2), 342.32(2), and 326.96(3) Å^3, respectively.

[c]The weighted average chemical composition for S^*_{3C} and S^*_{3D} was approximately estimated to be $PbCr_{0.4}S_{0.6}O_4$ and $PbCr_{0.2}S_{0.8}O_4$, respectively.

Table 2. Details of original paintings and corresponding embedded paint micro-samples investigated by means of Raman spectroscopy

Painting name and corresponding sample name/number	Van Gogh Museum inventory number	Creation date, technique, and sizes	Notes on past restoration treatments[6]	Chrome yellow composition[a]
Sunflowers gone to seed; sample F377/2 (Fig. S2 of Supporting Information)	Inv. n. S 121 V/1962	Mid-August to mid-September 1887; oil on cotton; 21.2 × 27.1 cm	The painting was wax-resin lined and varnished by J. C. Traas in the winter of 1926–1927. In 2003, the picture was cleaned and restored by E. Hendriks, removing the deteriorated old varnish layer. A very thin layer of Regalrez 1094 varnish was applied at the end of the restoration process.	Monoclinic $PbCrO_4$[b]
Bank of the Seine; sample F293/3 (Fig. S3 of Supporting Information)	Inv. n. S 77 V/1962	Mid-May to late July 1887; oil on linen; 32.0 × 46.0 cm	The painting was wax-resin lined and varnished by J. C. Traas sometime in the period 1927–1933. In 2005, the picture was cleaned and restored by E. Hendriks, removing the deteriorated old varnish layer. No new surface coating was applied.	Monoclinic $PbCr_{1-x}S_xO_4$ ($x \sim 0.1$) and/or monoclinic $PbCrO_4$[c]
Portrait of Gauguin; sample ×448/2 (Fig. S4 of Supporting Information)	Inv. n. S 257 V/1962	December 1888; oil on jute; 37 × 33 cm	In 1927, the canvas (without tacking margins) was stuck onto triplex using a whitish adhesive by J. C. Traas. The picture has never been varnished, which is quite exceptional.	Monoclinic and possible orthorhombic $PbCr_{1-x}S_xO_4$ ($x \sim 0.5$)

[a]A good agreement between the Raman profiles collected from selected areas of the painting using the portable device and those obtained from the corresponding paint micro-samples by means of the bench-top instrumentation was obtained (see par. 'Microinvasive and noninvasive identification of different chrome yellow types on works of art' for further details).

[b]Chrome yellow found in mixture with zinc yellow ($K_2O{\cdot}4ZnCrO_4{\cdot}3H_2O$).

[c]Chrome yellow sometimes found in mixture with chrome orange [$(1-x)PbCrO_4{\cdot}xPbO$] or vermilion (HgS).

The prevention of any laser-induced damage at the surface of works of art is a fundamental issue with noninvasive Raman studies; thus, with the aim of collecting the spectral signatures from laser-induced degradation products that might be formed *in situ*, additional tests were performed on the oil paint model made up of monoclinic $PbCrO_4$. For this purpose, excitation at 532.0 and 785.0 nm was used, considering that these two wavelengths are commonly implemented in portable Raman devices.[25,26] A power up to *ca.* 11 mW, an exposure time between 1–5 s and up to a maximum of 400 scans were employed.

In experimental conditions similar to those used for the paint models, spectra at 785.0 nm were collected from the original embedded paint micro-samples. Investigations using an excitation at 532.0 nm were performed on F377/2, because the deep red line was not available when this sample was analyzed.

The mathematical treatment of the micro-Raman spectra acquired from the paint models at 532.0 and 785.0 nm was performed by means of the Origin 8.0 software. The deconvolution process was performed using Lorentzian functions and employing the minimum number of components. The fitting results were characterized by squared regression coefficient values $R^2 > 0.994$.

Portable Raman

Measurements on paint model samples and on the paintings by Van Gogh were performed with a custom-made spectrophotometer equipped with a diode laser source emitting at 785.0 nm. The laser radiation was focused through an optical fiber (diameter of 105 μm) into an external probe. The backscattered Raman light was collected by a second optical fiber (diameter of 200 μm) and led to a Czerny–Turner polychromator (about 100 mm focal length) of a compact ORIEL MS125 spectrograph. This latter component was equipped with a 1024 × 128 pixel ANDOR charge coupled device detector kept at −46 °C with a Peltier cooler. A 1200 lines/mm grating was used during the analysis. Spectra were recorded in the 1850–200 cm^{-1} energy range. For the paint models, the maximum laser power at the sample was 30 mW, while on the original paintings, up to 10 mW was employed. The exposure time varied between 1 and 2 s, using 3–5 accumulations. The spectral resolution was about 4 cm^{-1}.

Results and discussion

Characterization of synthesized lead chromate-based compounds

Effect of the laser excitation wavelength

As described by several studies,[27–30] the bands at about 840 and 358 cm^{-1}, assigned to the chromate totally symmetric stretching (ν_1) and symmetric bending (ν_4) modes, respectively,[31,32] can be used as marker signals for a generic identification of chrome yellow pigments in works of art. We have previously reported[23] that the characterization of different varieties of lead chromate compounds can be obtained considering the position, band-shape and relative intensity of both the symmetric and asymmetric bending modes (ν_4 and ν_2) positioned in the 420–300 cm^{-1} energy range. Additionally, the detection of the sulfate symmetric stretching mode (ν_1) at *ca.* 970 cm^{-1} provides indications about the presence of $PbCr_{1-x}S_xO_4$ compounds.

Chromate salts are known to show a resonance Raman effect that gives rise to a significant enhancement of the totally symmetric stretching band [$\nu_1(CrO_4^{2-})$] when the excitation wavelength is in resonance with the energy of the lowest allowed ligand-to-metal charge transfer transition.[33] Figure 1 illustrates the Raman spectra of the samples S_{1mono}, S_{3A}–S_{3D} ($PbCr_{1-x}S_xO_4$), and S_{1ortho} obtained at four different excitation lines (785.0, 532.0, 514.5, and 488 nm). With decreasing excitation wavelength, the intensity of the $\nu_1(CrO_4^{2-})$ band is enhanced with respect to the bending $\nu_2/\nu_4(CrO_4^{2-})$ bands as a result of the resonance Raman effect.[33–35] Indeed, the UV-visible spectrum of $PbCrO_4$ reported in Fig. S5 (Supporting Information) shows a broad absorption band centered around 400 nm that is related to a ligand-to-metal charge transfer band responsible for the yellow color.

It follows that in the spectra acquired at 488 nm [Fig. 1(d)], the intensity of the bending modes (420–300 cm^{-1}) is very low, so that no useful information can be obtained that allows to properly characterize the different lead chromate compounds. Moreover, at this wavelength, the $\nu_1(SO_4^{2-})$ vibration (*ca.* 978 cm^{-1}) is only visible in the profile of the sample with the highest sulfate content (S_{3D}).

Regarding the spectra collected at 514.5 nm [Fig. 1(c)], the presence of the $\nu_1(SO_4^{2-})$ band as well as the broader shape and different position of the $\nu_2/\nu_4(CrO_4^{2-})$ modes only distinguish the profiles of the orthorhombic $PbCrO_4$ (S_{1ortho}) and the more S-rich $PbCr_{1-x}S_xO_4$ coprecipitates (S_{3C} and S_{3D}) with respect to those of the monoclinic compounds (S_{1mono}, S_{3A}, and S_{3B}).

Regardless of the sulfate amount present, in case of the spectra obtained either using 532.0 [Fig. 1(b)] or 785.0 nm [Fig. 1(a)] excitation, the band-shape and position of the chromate bending modes allow different chrome yellow types to be readily distinguished (cf. Section 'Raman band component analysis' for a detailed discussion). However, in case of the profiles collected at 532.0 nm, the differentiation between S_{1mono} and S_{3A} is not possible, because of the absence of the $\nu_1(SO_4^{2-})$ mode in the spectrum of the latter sample.

It can be concluded that using the 785.0 nm line and working in nonresonant mode, a higher information content can be obtained that allows to discriminate among different chrome yellow types. Consistent with the literature,[29] we also observed that a minor fluorescence background contribution because of the binding medium affects the profiles when the deep red excitation is employed in comparison to the ones recorded at shorter wavelengths.

As we discussed in a previous work,[23] the same systematic differences observed at 785.0 nm with the bench-top Raman instrument [Fig. 1(a)] are appreciable in the scattering profiles collected with the portable device at the same excitation wavelength, despite its lower instrumental spectral resolution.

Laser-induced damage tests

Figure 2 shows the spectra resulting from laser-induced damage tests that were carried out on S_{1mono} at 532.0 and 785.0 nm at different exposure times and laser power settings.

Regarding the spectra collected using 532.0 nm excitation [Fig. 2(a)], when the laser power is kept at *ca.* 1 mW, no changes of the spectral features are observable varying the exposure time (between 1 and 5 s) and increasing the number of scans collected at the same point (up to 100 scans total).

At 3 mW, a broadening of the spectral features occurs in the entire spectral range along with a modification of the relative

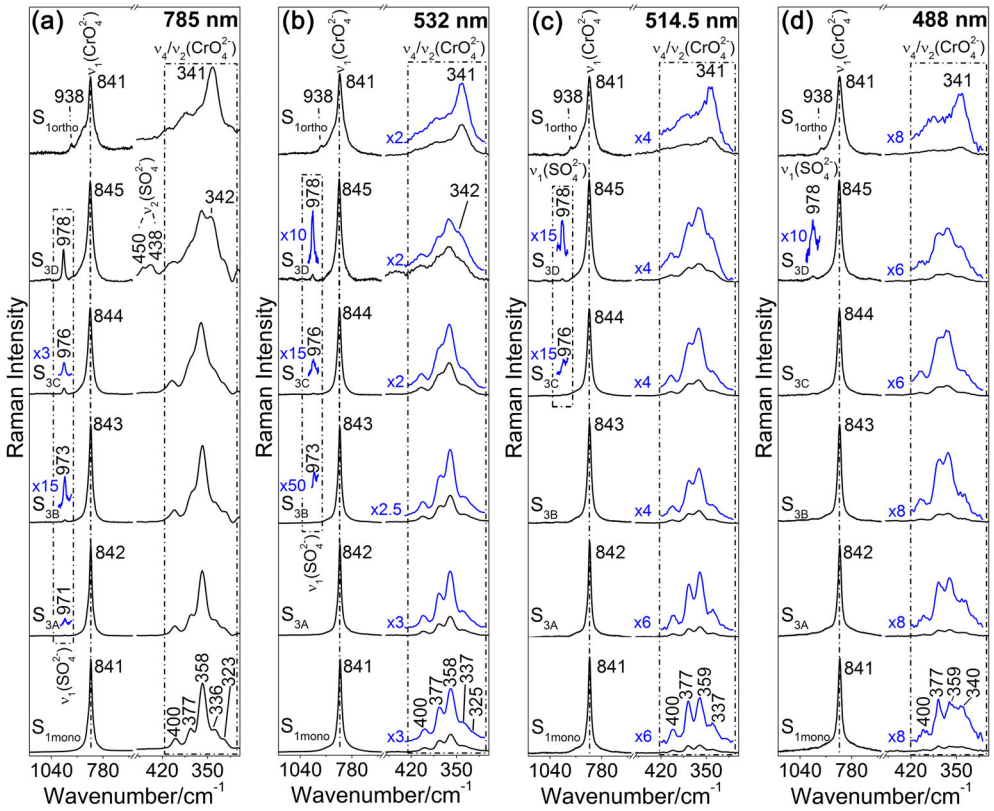

Figure 1. Raman spectra of paint model samples of $PbCrO_4$ (S_{1mono}, S_{1ortho}) and $PbCr_{1-x}S_xO_4$ (S_{3A}-S_{3D}) collected by means of the bench-top instrumentation at the following excitation wavelengths: (a) 785.0 nm (power: 3–7 mW; exposure time: 5–10 s; 5–10 scans); (b) 532.0 nm (power: 1 mW; exposure time: 3–10 s; 5–25 scans); (c) 514.5 nm (power: 0.6–0.7 mW; exposure time: 2–4 s; 10–40 scans); and (d) 488.0 nm (power: 0.6–0.7 mW; exposure time: 1–4 s; 20–30 scans). See the work of Monico *et al.*[23] for the spectra acquired by means of the portable device at 785 nm.

intensities of the bending modes, although no significant changes of the position of the $\nu_1(CrO_4^{2-})$ and $\nu_2/\nu_4(CrO_4^{2-})$ bands are observable.

New spectral features, ascribable to the formation of Cr(III) oxide-based compounds,[36,37] appear in the spectra acquired at 6 and 11 mW. In particular, at 6 mW the Raman frequency of the $\nu_1(CrO_4^{2-})$ mode shifts from 839 to 827 cm^{-1} with increasing scans number (exposure time 1 s) and after 15 scans a new band at *ca.* 541 cm^{-1} appears. The latter signal is assignable to the Cr (III)-O stretching mode.[36,37] At 11 mW, signals ascribable to Cr_2O_3 (535–541, 340, and 305 cm^{-1}) appear just after 1 scan (exposure time 1 s); their intensity decreases with increasing number of scans, most probably due to the formation of an amorphous phase.[37]

Figure 2(b) illustrates that no changes are observable in the spectrum of S_{1mono} when the power of the 785.0 nm laser at the sample is kept at 7 mW (maximum value reachable with the available experimental setup). An increase of either the exposure time (from 1 to 10 s) or the number of scans at the same point (up to 300) does not give rise to observable modifications of the spectral features. As Fig. S6 (Supporting Information) illustrates, measurements performed on samples S_{3B}, S_{3C}, and S_{3D} by means of the portable device and using higher laser power (up to 24 mW) show similar stable results.

On the basis of these observations, we can conclude that the advantage to use an excitation wavelength not absorbed by the pigment (i.e. 785.0 nm) not only resides with the possibility to gain detailed and complete information on the different types of lead chromate pigments but also allows avoiding a laser-induced photochemical reduction.

Raman band component analysis

In order to find reliable spectral makers of the different chrome yellow forms, a Raman band component analysis was applied to the Cr–O stretching and bending regions of the spectra collected using a 785.0 nm excitation (nonresonant spectra). Similar results are obtained for spectra collected at 532.0 nm, and those obtained in the Cr–O bending energy range are shown in Fig. S7 (Supporting Information).

Consistent with the literature,[31,32] three components accurately describe the Cr–O stretching modes for all samples, except in case of S_{1ortho}, for which an additional weak component at 938 cm^{-1}, ascribable to the asymmetric stretching (ν_3) of polychromate-species,[38] is required in order to obtain a good fitting result [Fig. 3(a)].

When increasing the sulfate concentration, the wavenumber of the $\nu_1(CrO_4^{2-})$ mode monotonically increases from 841 cm^{-1} for lead chromate (S_{1mono} and S_{1ortho}) to 845 cm^{-1} for S_{3D} [Fig. 4(a), on top]. Also, the full width at half maximum of both these components increases (e.g., for the most intense component at 841–845 cm^{-1}, from about 15 cm^{-1} for S_{1mono} to *ca.* 25 cm^{-1} for S_{3D}). Consistent with the XRD data (Table 1 and Fig. S1 of Supporting Information) and with previous studies on other $MCr_{1-x}S_xO_4$ compounds (M = Ba, Ca, Sr, Pb, and Na),[39–41] these observations can be explained taking into account the lattice

Journal of RAMAN SPECTROSCOPY

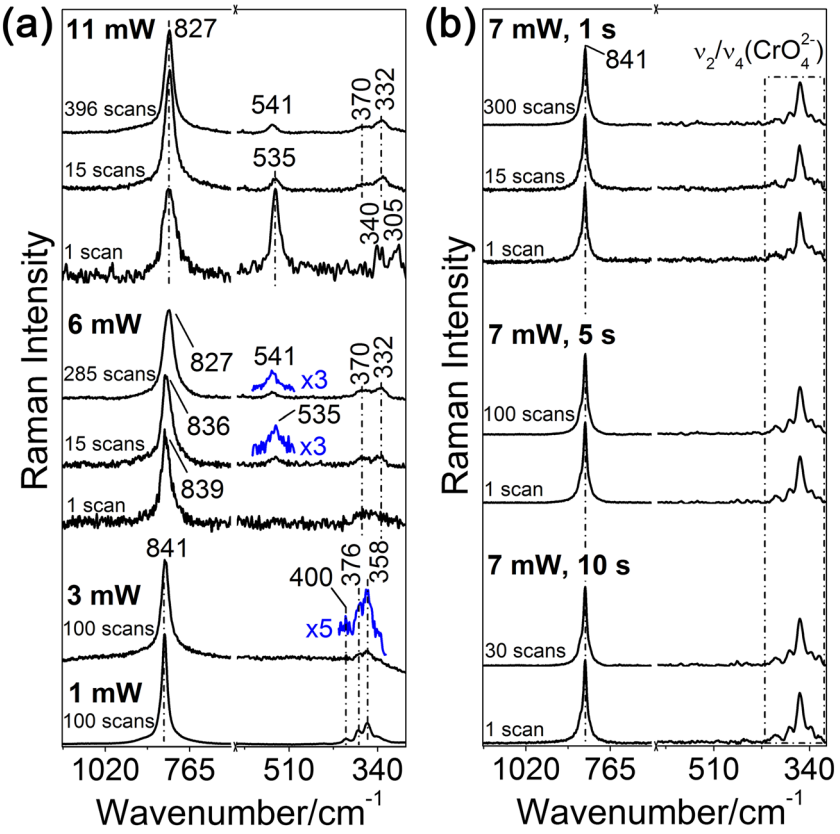

Figure 2. Raman spectra of paint model sample of monoclinic $PbCrO_4$ (S_{1mono}) collected by means of the bench-top instrumentation at different power and/or exposure time: (a) 532.0 nm (1–11 mW, exposure time: 1 s) and (b) 785.0 nm (7 mW, exposure time: 1–10 s) (see text for further details). In Fig. S6 (Supporting Information), similar experiments performed by means of the portable instrumentation are reported.

compression effect. Also, the changes in the band-shape, more symmetrical at low sulfate content, must be considered in this sense. As observed for the chromate anion vibrations, the lattice compression effect determines a shift of the Raman frequency of the $\nu_1(SO_4^{2-})$ mode as a function of increasing sulfate amount [Fig. 4(a), on middle]: its energy position moves from 971 cm^{-1} for S_{3A} to 980 cm^{-1} for $PbSO_4$ (spectrum not reported). Only in case of the most S-rich sample S_{3D}, additional signals at 450 and 438 cm^{-1} ascribable to the sulfate bending modes [$\nu_2(SO_4^{2-})$] are visible [Fig. 1(a)].

According to the literature,[31,32] in the Cr–O bending region (420–300 cm^{-1}), four to five components are generally required to obtain good fitting results [Fig. 3(b)]. For S_{1mono}, the $\nu_4/\nu_2(CrO_4^{2-})$ modes are located at 400, 377, 358, 336, and 323 cm^{-1}. As observed for the components describing the Cr–O stretching region, also those ascribed to the chromate bending modes show an increase of full width at half maximum (e.g., for the component at 358–360 cm^{-1}, from about 13 cm^{-1} for S_{1mono} to *ca*. 21 cm^{-1} for S_{3D}), a change of the relative intensities and a progressive shift of the centroid position toward higher energy with increasing sulfate abundance. As an example, Fig. 4(a) (bottom) shows the Raman frequency of the $\nu_4(CrO_4^{2-})$ mode at 400–410 cm^{-1} *versus* the sulfate concentration.

Interestingly, the chromate bending modes of S_{1ortho} show features that are different from those of S_{1mono}, both in terms of number, position, and relative intensity of the fitting components. Consistent with Davies *et al.*,[42] the bending band-shape of S_{1ortho} resembles that of other orthorhombic chromate salts. The spectrum of this compound is properly described including four components in the fitting model, located at 411, 384, 362, and 341 cm^{-1}. As Fig. 3(b) illustrates, the band located at 341 cm^{-1} appears to be characteristic for the presence of an orthorhombic crystalline phase: its contribution is only significant in case of S_{3D} and S_{1ortho}. On the other hand, the intensity of the signal located in the 358–362 cm^{-1} wavenumber range is related to the presence of the monoclinic phase. The ratio of the net area of the latter component and that of the band located between 336 and 341 cm^{-1} [Fig. 4(b), bottom panel] decreases monotonically with the percentage amount of orthorhombic phase (as estimated by XRD; cf. Table 1), thus confirming in a semi-quantitate manner the aforementioned observations. A similar trend is also visible plotting the ratio of net area of the Cr–O symmetric (841–845 cm^{-1}) and the asymmetric (857–880 cm^{-1}) stretching components [Fig. 4(b), top panel].

Mixtures of different chrome yellow types

Figure 5 illustrates the Raman spectra acquired from the model paints prepared mixing S_{1mono} ($PbCrO_4$) and either S_{3B} ($PbCr_{0.75}S_{0.25}O_4$) or S_{3D} ($PbCr_{0.2}S_{0.8}O_4$) in different proportions. Considering that mixtures of different chrome yellow varieties may be encountered on original works of art, spectra were acquired not only employing the bench-top instrument (black lines) but also the portable device (red lines).

As shown in Fig. 5 (black lines), in the spectra collected from mixture paints containing a mass fraction of S_{1mono} equal or higher than that of S_{3B} or S_{3D} (see spectra corresponding to S_{1mono}:S_{3B}/S_{3D} = 1 : 1, 3 : 1, and 9 : 1), the chromate stretching and bending modes resemble to that of S_{1mono} [cf. Fig. 1(a)]. This

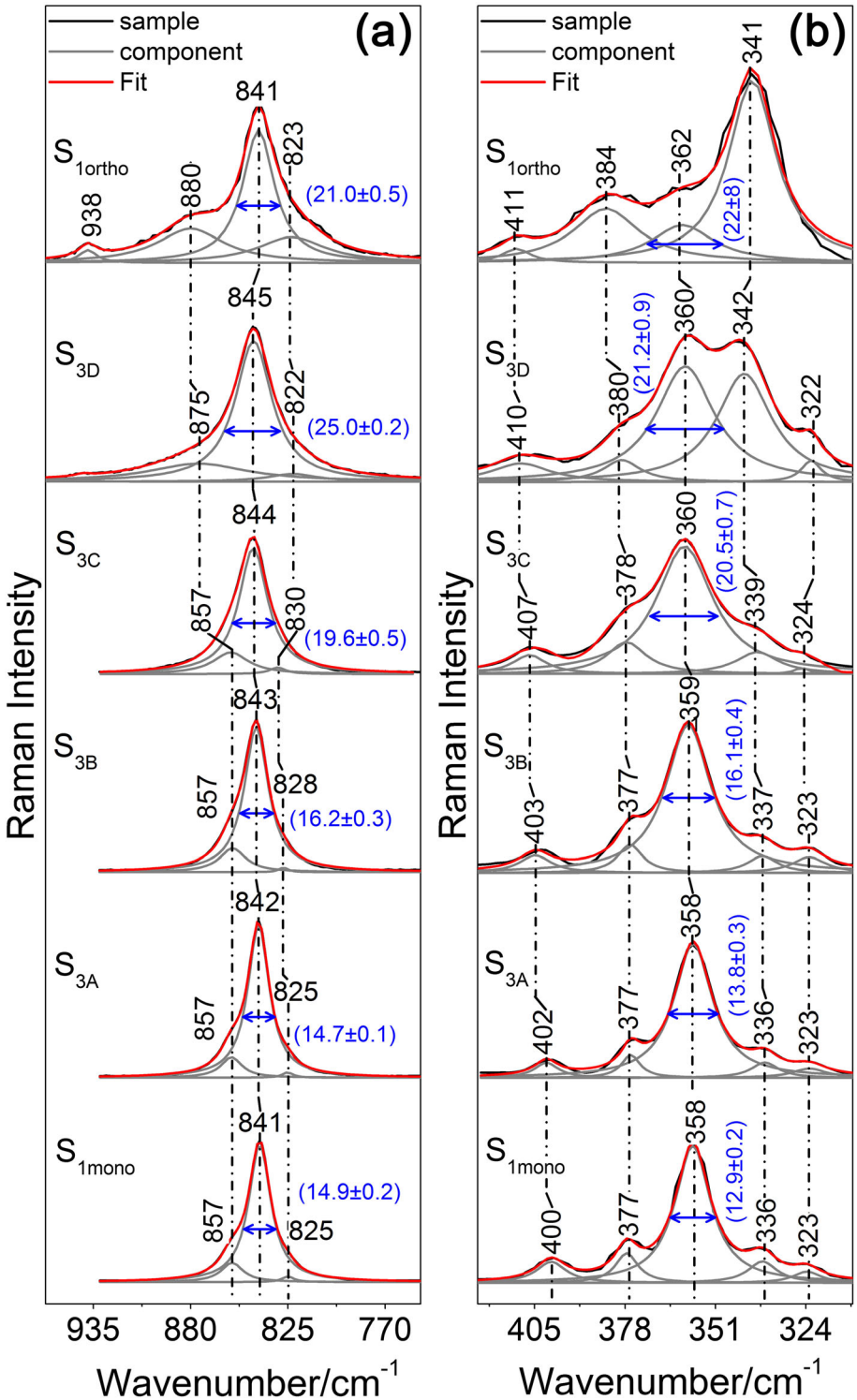

Figure 3. Chromate (a) stretching and (b) bending region of the Raman spectra acquired at 785.0 nm from paint model samples of $PbCrO_4$ (S_{1mono}, S_{1ortho}) and $PbCr_{1-x}S_xO_4$ (S_{3A}–S_{3D}) and corresponding results of the band component analysis. Black labels indicate the wavenumber positions of each components, while in blue the full width at half maximum (FWHM) values for the band at 841–845 cm^{-1} and 358–362 cm^{-1} are shown. (This figure is available in colour online at wileyonlinelibrary.com/journal/jrs.)

is demonstrated by the position of the $\nu_1(CrO_4^{2-})$ vibration at 841 cm^{-1} and those of the $\nu_2/\nu_4(CrO_4^{2-})$ signals at 400 and 358 cm^{-1}. It follows that for this group of paint samples, the S_{3B} or S_{3D} coprecipitates can be identified only by the presence of the $\nu_1(SO_4^{2-})$ mode (at 973 and 978 cm^{-1}, respectively). The detection of $PbCr_{1-x}S_xO_4$ is not possible when S_{1mono} and either S_{3B} or S_{3D} are mixed in a 9 : 1 weight ratio (Fig. 5, spectra S_{1mono} : S_{3B}/S_{3D} = 9 : 1). The $\nu_1(SO_4^{2-})$ signal of S_{3B} starts to become visible when the mass fraction of the coprecipitate becomes more or less equal to that of S_{1mono} [Fig. 5(a), see spectrum corresponding to S_{1mono} : S_{3B} = 1 : 1]. This band is already detectable in the spectrum when S_{1mono} and S_{3D} are mixed in a 3 : 1 weight ratio

Journal of RAMAN SPECTROSCOPY

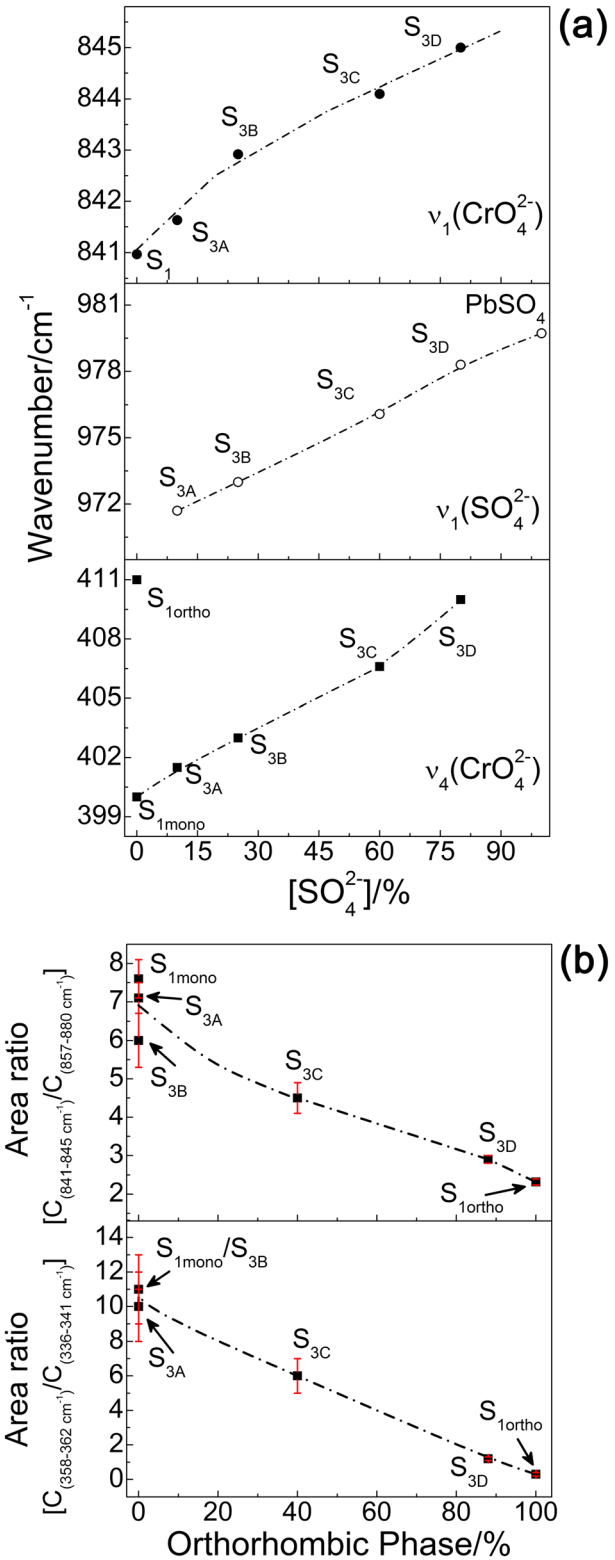

Figure 4. (a) Plot of the Raman frequencies of (from top to bottom): $\nu_1(CrO_4^{2-})$ (filled circles) $\nu_1(SO_4^{2-})$ (empty circles), and $\nu_4(CrO_4^{2-})$ (squares) *versus* the percentage amount of sulfate. (b) Net area ratio between the Raman components positioned (top) at 841–845 cm^{-1} and 857–880 cm^{-1} and (bottom) at 358–362 cm^{-1} and 336–341 cm^{-1} *versus* the percentage amount of orthorhombic phase.

[Fig. 5(b), spectrum corresponding to $S_{1mono}:S_{3D}=3:1$]. It is worth to underline that the symmetric stretching of sulfate in the lead chromate structure is shifted toward lower wavenumbers with respect to pure lead sulfate [see Section 'Raman band component analysis' and Fig. 4(a)]. However, the eventual presence of anglesite in the paint may hinder the identification of S_{3B} or S_{3D} coprecipitates in mixture with S_{1mono}.

When the relative amount of S_{3B} exceeds that of S_{1mono} [Fig. 5 (a), spectra corresponding to $S_{1mono}:S_{3B}=1:3$ and $1:9$], the spectral features become progressively more similar to that of the pure S_{3B} compound. This is demonstrated by a shift toward higher wavenumbers of the $\nu_1(CrO_4^{2-})$ (843 cm^{-1}) and $\nu_2/\nu_4(CrO_4^{2-})$ modes (403 and 359 cm^{-1}) as well as a gradual increase of the intensity of the $\nu_1(SO_4^{2-})$ vibration.

Except for the presence of the $\nu_1(SO_4^{2-})$ band at 978 cm^{-1}, the identification of S_{3D} is difficult even in the mixture samples containing the lowest mass fraction of S_{1mono} [Fig. 5(b), spectra corresponding to $S_{1mono}:S_{3D}=1:3$, and $1:9$]. The chromate and stretching bands mostly resemble that of S_{1mono}: the $\nu_1(CrO_4^{2-})$ band is positioned at 841 cm^{-1} and only a slight shift of the $\nu_4(CrO_4^{2-})$ frequencies takes place (402 and 359 cm^{-1}). The characteristic band of S_{3D} located at 342 cm^{-1} appears as a weak feature. Only in the spectrum collected from the sample obtained mixing S_{1mono} and S_{3D} in a 1:9 weight ratio [Fig. 5(b), spectrum corresponding to $S_{1mono}:S_{3D}=1:9$] the $\nu_2(SO_4^{2-})$, the vibrations at 450 and 438 cm^{-1} are visible.

As Fig. S8 (Supporting Information) illustrates, the aforementioned results can be justified by taking into account the Raman scattering coefficient of the lead chromate compounds. Its value progressively decreases as a function of both the relative amounts of sulfate and of the orthorhombic phase.

In the $\nu_1(CrO_4^{2-})$ and $\nu_1(SO_4^{2-})$ regions, the spectra obtained by means of the portable Raman spectrometer (Fig. 5, red lines) show features that are comparable to those acquired using the bench-top instrument. The lower instrumental spectral resolution makes a detailed characterization of the bands located in the Cr–O bending region more difficult. However, with the increase of the relative amount of S_{3B} or S_{3D}, a broadening of the $\nu_2/\nu_4(CrO_4^{2-})$ modes becomes appreciable.

On the basis of these investigations, it follows that detection problems may be encountered when different lead chromate-based compounds are present together, because of the predominance in the Raman profiles of the spectral features of the monoclinic $PbCrO_4$ and S-poor $PbCr_{1-x}S_xO_4$, which have a higher Raman scattering coefficient with respect to the corresponding compounds containing orthorhombic crystalline phases and higher amounts of sulfur.

Microinvasive and noninvasive identification of different chrome yellow types on works of art

The comparison between the micro-Raman spectra collected from the yellow areas of the embedded paint micro-samples F377/2, F293/3, and ×448/2 [Fig. 6(b), black lines] and those obtained from the model paints [Fig. 6(b), gray lines] clearly demonstrate the presence of different chrome yellow forms. As we described in a previous work,[23] this result is also confirmed by synchrotron radiation-based micro-XRD and reflection mid-infrared investigations.

Noninvasive *in situ* Raman measurements allowed similar information to be obtained analyzing different areas of yellow paint of Van Gogh paintings *Sunflowers gone to seed*, *Bank of the Seine*,

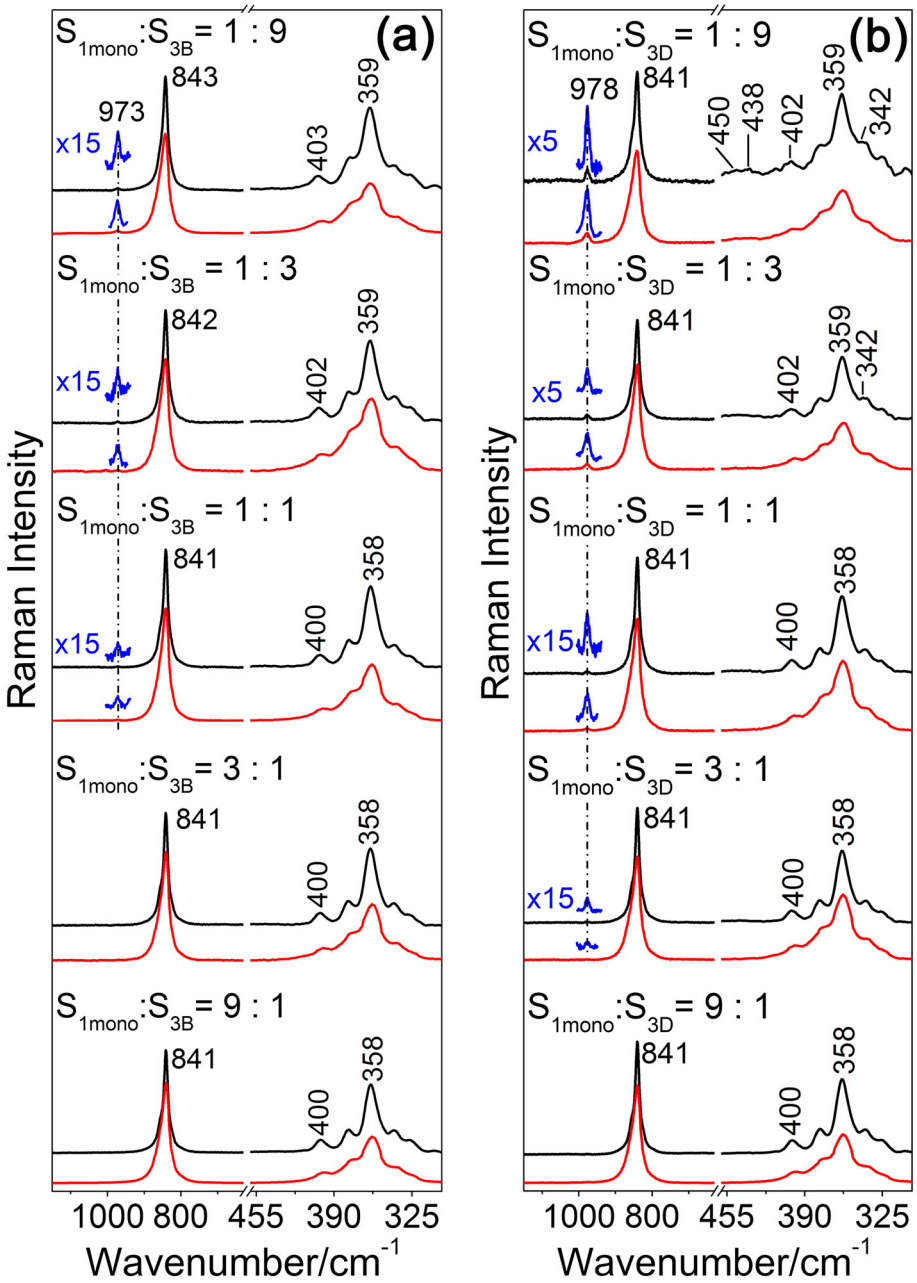

Figure 5. Raman spectra of paint models containing different proportions of monoclinic $PbCrO_4$ (S_{1mono}) and either (a) $PbCr_{0.75}S_{0.25}O_4$ (S_{3B}) or (b) $PbCr_{0.2}S_{0.8}O_4$ (S_{3D}) acquired using a 785.0 nm excitation of (black) bench-top and (red) portable devices. (This figure is available in colour online at wileyonlinelibrary.com/journal/jrs.)

and *Portrait of Gauguin* at the Van Gogh Museum (see Table 2 for further details about these paintings).

The sampling regions of the cross-sections reported in Fig. 6(a) and the locations where the *in situ* Raman spectra of Fig. 6(c) were acquired are illustrated in the Supporting Information (Figs S2–S4).

In sample F377/2, taken from *Sunflowers gone to seed*, the micro-Raman spectrum acquired from a yellow-orange crystal [Fig. 6(b), spectrum 01] shows the presence of monoclinic $PbCrO_4$. As reported in Fig. S9a (Supporting Information), similar investigations carried out on a greenish yellow pigment grain (spectrum 02) allowed also the presence of the zinc yellow pigment ($K_2O{\cdot}4ZnCrO_4{\cdot}3H_2O$) to be identified (signals at 941, 893, and 872 cm^{-1}).

During the last restoration treatment of the painting, a thin layer of Regalrez 1094 varnish (a hydrogenated oligomer of styrene and α-methyl styrene) was rubbed onto the surface, just enough to saturate dark color areas while retaining a matt effect that was in keeping with the artist's intention (see Table 2 for details). Despite the presence of this varnish layer, a proper characterization of the paint layer underneath could be obtained by means of *in situ* Raman measurements: the spectrum collected from a greenish yellow area [Fig. 6(c), spectrum SFS04], shows spectral features that resemble those of the monoclinic $PbCrO_4$. The additional presence of a signal at 872 cm^{-1} can be ascribed to the presence of zinc yellow (see Fig. S2 of Supporting Information for the location where this spectrum was acquired).

Journal of RAMAN SPECTROSCOPY

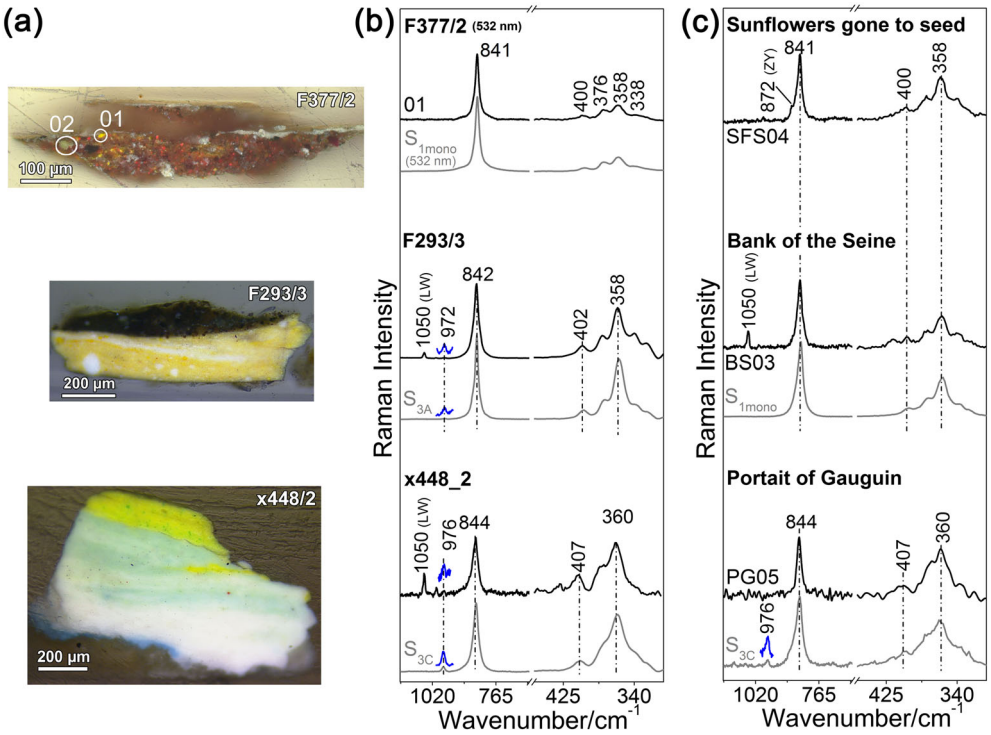

Figure 6. (a) Optical microscope images and (b) corresponding Raman spectra collected from yellow areas of (from top to bottom) the original embedded paint micro-samples F377/2, F293/3 (both samples were taken before varnish removal/samples include varnish layer) and ×448/2 taken from paintings by Vincent van Gogh. (c) Noninvasive in situ Raman spectra collected from the corresponding Van Gogh paintings (from top to bottom) *Sunflowers gone to seed*, *Bank of the Seine*, and *Portrait of Gauguin*. In (a) the locations where the spectra of (b) were obtained are indicated by white circles and labels. The spectrum 02 collected from F377/2 is reported in Fig. S9a (Supporting Information). The sampling areas of the cross-sections reported in (a) and the *in situ* measurement locations of the spectra shown in (c) are illustrated in Figs S2–S4 (Supporting Information). (This figure is available in colour online at wileyonlinelibrary.com/journal/jrs.)

In the case of sample F293/3, originating from *Bank of the Seine*, the lighter-yellow regions show the presence of a $PbCr_{1-x}S_xO_4$ coprecipitate having spectral features close to that of the reference compound S_{3A}. In this sample, lead white was also identified (signal at 1050 cm^{-1}).[43] Consistent with the data obtained from F293/3, the noninvasive Raman spectrum collected from a yellow painted area of the corresponding painting (Fig. S3, Supporting Information) also reveals the presence of lead white [Fig. 6(c), spectrum BS03]. Although the yellow pigment shows Raman features that are very close to that of a monoclinic lead chromate-based compounds (e.g., S_{1mono}, S_{3A}), a more certain identification of its chemical composition as either $PbCrO_4$, $PbCr_{1-x-}S_xO_4$ ($x \leq 0.25$) or a mixture of both of them is difficult to make, in view of the absence of the $\nu_1(SO_4^{2-})$ feature in the spectrum. The relative low power of the laser (8–10 mW) that was used during the analysis may be responsible for this uncertainty. As Fig. S6 (Supporting Information) illustrates, preliminary Raman tests performed on the model paints using the portable device revealed that for the monoclinic $PbCr_{1-x}S_xO_4$, the $\nu_1(SO_4^{2-})$ band only becomes clearly visible when a laser power above *ca.* 20 mW is employed.

Regarding the sample *x*448/2 taken from *Portrait of Gauguin*, the chrome yellow pigment was identified as S-rich $PbCr_{1-x}S_xO_4$ ($x \sim 0.5$). As Fig. 6(b) illustrates, the micro-Raman spectrum collected from the light yellow areas shows features that resemble those of the reference compound S_{3C}. The additional presence of a signal at 1050 cm^{-1} indicates the presence of lead white. Consistent with the micro-Raman results collected from the embedded sample, the identification of a chrome yellow type similar to S_{3C} is also confirmed by *in situ* Raman spectroscopy [Fig. 6(c), spectrum PG05].

Again, the absence of the $\nu_1(SO_4^{2-})$ signal can be ascribed to the relative low power of the laser that was used during the analysis (cf. Fig. S6 of Supporting Information).

In addition, as Fig. S9b (Supporting Information) illustrates, the chrome orange pigment [(1−x)$PbCrO_4$·xPbO] was identified to be the main constituent compound of some of the orange painted areas of the paintings *Bank of the Seine* and *Portrait of Gauguin*. In some reddish-orange areas of the former painting, the presence of vermilion (HgS, most intense signal at *ca.* 252 cm^{-1})[43] was found to be present in a mixture with chrome orange.

Conclusions

In $PbCr_{1-x}S_xO_4$ solid solutions, the substitution of the chromate ions by smaller sulfate ions leads to a volume decrease of the monoclinic unit cell at low sulfate concentration and a change of the crystalline structure from monoclinic to orthorhombic at high sulfate concentration. These changes affect to a different extent all the fundamental vibrational bands of these materials. In particular, the chromate bending multiplet (ν_2/ν_4) is strongly affected by the chromate/sulfate substitution, showing a shift of band positions as a function of the cell compression and a clear modification of band shapes related to the change of the crystalline structure. Additionally, the ν_1 symmetric stretching band of both sulfate and chromate ions shift slightly toward higher energy as a function of the sulfate concentration. Another relevant effect of the chromate to sulfate substitution is a decrease of the Raman scattering cross-section.

The spectral profiles of these pigments are dependent on the Raman excitation energy: both in resonance (at 488.0 nm) and pre-resonance (at 514.5 nm) mode, a strong enhancement of the totally symmetric stretching chromate mode (ν_1) with respect to the bending modes is observed. Despite increasing the sensitivity of Raman spectroscopy and thus facilitating the generic identification of chromate pigments, the resonance mode reduces its specificity, therefore rendering a reliable recognition of different solid solution forms more difficult. On the other hand, the nonresonant mode of excitation (at 785.0 nm) allows for a clear detection of both the chromate bending profile and the sulfate stretching band, also in the S-poorer $PbCr_{1-x}S_xO_4$ ($x \leq 0.25$) solid solutions. In addition, working at 785.0 nm avoids any photochemical damage to the pigment; such damage is clearly observed when 532.0 nm or higher energies are employed for excitation. The portable set-up equipped with a 785.0 nm diode laser and a fiber optic probe proved to have enough spectral resolution and sensitivity for a reliable identification of the six different chrome yellow solid solutions prepared as oil paint models. It must be underlined that due to the decrease of the scattering coefficient with increasing sulfate and orthorhombic phase abundance, the detection of a small amount of S-rich $PbCr_{1-x}S_xO_4$ in mixtures with monoclinic lead chromate as main constituent can be difficult, especially when working at low laser powers.

Noninvasive Raman spectroscopy has been successfully exploited to study *in situ* the yellow palette of three Van Gogh paintings. The results, validated by a micro-Raman investigation of a few available cross-sections, convincingly demonstrates that Van Gogh employed different type of lead chromate/sulfate solid solutions, either in undiluted form or in mixtures with other pigments (such as lead white and vermilion). He also used other chromate-based materials such as chrome orange [(1−x) $PbCrO_4$·xPbO] and zinc yellow (K_2O·4$ZnCrO_4$·3H_2O).

This paper shows that noninvasive Raman spectroscopy is a reliable and sensitive tool for identifying and mapping different types of chrome yellow on the surface of works of art, thus contributing to advance our understanding on the causes of alteration of this class of pigments.

Acknowledgements

This research was supported by Interuniversity Attraction Poles Programme - Belgian Science Policy (S2-ART project S4DA) and also presents results from GOA 'XANES meets ELNES' (Research Fund University of Antwerp, Belgium), FWO (Brussels, Belgium) projects no. G.0704.08 and G.01769.09. Support from the Italian projects PRIN (SICH Sustainability in Cultural Heritage: from diagnosis to the development of innovative system for consolidation, cleaning and protection) and PON (ITACHA Italian advanced technologies for cultural heritage applications) is also acknowledged. The analysis of the paintings *Sunflowers gone to seed*, *Bank of the Seine*, and *Portrait of Gauguin* was performed within the mobile laboratory access activity of the FP7 programme CHARISMA supported by EC (Grant Agreement 228330). LM acknowledges the Italian National Research Council (CNR) for the financial support in the framework of the Short Term Mobility Programme 2013. Thanks are expressed to Muriel Geldof, Cultural Heritage Agency of The Netherlands, for selecting and sharing the information on the cross-sections and to the staff of the Van Gogh Museum for the agreeable cooperation.

References

[1] J. H. Townsend, *Stud. Conserv.* **1993**, *38*, 231.
[2] S. Cove, in Constable, (Eds.: L. Parris, I. Fleming-Williams), Tate Gallery, London, **1991**, pp. 493–518.
[3] D. Bomford, J. Kirby, J. Leighton, A. Roy, Art in the Making: Impressionism, National Gallery Publications, London, **1990**, p. 158.
[4] M. H. Butler, *Bull. Am. Inst. Conserv. Historic Artistic Works* **1973**, *13*, 77.
[5] P. Dredge, R. Wuhrer, M. R. Phillips, *Microsc. Microanal.* **2003**, *9*, 139–143.
[6] E. Hendriks, M. Geldof, in Vincent Van Gogh Paintings 2: Antwerp & Paris, 1885-1888, (Eds.: E. Hendriks, L. van Tilborgh), Waanders Publishers, Amsterdam and Zwolle, **2011**, pp. 90–143.
[7] L. Jansen, H. Luijten, N. Bakker, Vincent Van Gogh – The Letters, Thames & Hudson Ltd., London and Amsterdam, **2009** and www.vangoghletters.org (accessed on December 5, 2013).
[8] J. Kirby, K. Stonor, A. Roy, A. Burnstock, R. Grout, R. White, *Natl. Gallery Tech. Bull.* **2003**, *28*, 4.
[9] G. Van der Snickt, K. Janssens, O. Schalm, C. Aibéo, H. Kloust, M. Alfeld, *X-Ray Spectrom.* **2010**, *39*, 103.
[10] H. Kühn, M. Curran, in Artists' Pigments: A Handbook of Their History and Characteristics, vol. *1*, (Ed.: R. L. Feller), Cambridge University Press, **1986**, pp. 187–200.
[11] N. Eastaugh, V. Walsh, T. Chaplin, R. Siddall, Pigment Compendium—A Dictionary and Optical Microscopy of Historical Pigments, Elsevier, Oxford, **2004**.
[12] A. G. Abel, in Paint and Surface Coatings: Theory and Practice (2nd edn), (Eds.: R. Lambourne, T. A. Strivens), Woodhead Publishing Ltd, Cambridge, **1999**, pp. 91–165.
[13] H. Effenberger, F. Pertlik, *Z. Kristallogr.* **1986**, *176*, 75.
[14] R. M. James, W. A. Wood, *Proc. R. Soc., Ser. A* **1925**, *109*, 598.
[15] M. J. Crane, P. Leverett, L. R. Shaddick, P. A. Williams, J. T. Kloprogge, R. L. Frost, *N. Jb. Miner. Mh.* **2001**, *11*, 505.
[16] L. J. H. Erkens, H. Hamers, R. J. M. Hermans, E. Claeys, M. Bijnens, *Surf. Coat. Int., Part B* **2001**, *84*, 1969.
[17] R. J. Cole, *Paint Res. Ass. Tech. Pap.* **1955**, *199*, 1.
[18] V. Watson, H. F. Clay, *J. Oil Colour Chem. Assoc.* **1955**, *38*, 167.
[19] L. Monico, G. Van der Snickt, K. Janssens, W. De Nolf, C. Miliani, J. Verbeeck, H. Tian, H. Tan, J. Dik, M. Radepont, M. Cotte, *Anal. Chem. (Washington, DC, U. S.)* **2011**, *83*, 1214.
[20] L. Monico, G. Van der Snickt, K. Janssens, W. De Nolf, C. Miliani, J. Dik, M. Radepont, E. Hendriks, M. Geldof, M. Cotte, *Anal. Chem. (Washington, DC, U. S.)* **2011**, *83*, 1224.
[21] L. Monico, K. Janssens, C. Miliani, G. Van der Snickt, B. G. Brunetti, M. Cestelli Guidi, M. Radepont, M. Cotte, *Anal. Chem. (Washington, DC, U. S.)* **2013**, *85*, 860.
[22] H. Tan, H. Tian, J. Verbeeck, L. Monico, K. Janssens, G. Van Tendeloo, *Angew. Chem. Int. Ed.* **2013**, *52*, 3.
[23] L. Monico, K. Janssens, C. Miliani, B. G. Brunetti, M. Vagnini, F. Vanmeert, G. Falkenberg, A. Abakumov, Y. Lu, H. Tian, J. Verbeeck, M. Radepont, M. Cotte, E. Hendriks, M. Geldof, L. van der Loeff, J. Salvant, M. Menu, *Anal. Chem. (Washington, DC, U. S.)* **2013**, *85*, 851.
[24] C. Miliani, F. Rosi, B. G. Brunetti, A. Sgamellotti, *Acc. Chem. Res.* **2010**, *43*, 728.
[25] P. Vandenabeele, K. Castro, M. Hargreaves, L. Moens, J. M. Madariaga, H. G. M. Edwards, *Anal. Chim. Acta* **2007**, *588*, 108.
[26] F. Rosi, V. Manuali, T. Grygar, P. Bezdicka, B. G. Brunetti, A. Sgamellotti, L. Burgio, C. Seccaroni, C. Miliani, *J. Raman Spectrosc.* **2011**, *42*, 407.
[27] M. C. Caggiani, P. Colomban, *J. Raman Spectrosc.* **2011**, *42*, 790.
[28] S. Daniilia, D. Bikiaris, L. Burgio, P. Gavala, R. J. Clark, Y. Chryssoulakis, *J. Raman Spectrosc.* **2002**, *33*, 807.
[29] K. Castro, P. Vandenabeele, M. D. Rodríguez-Laso, L. Moens, J. M. Madariaga, *Anal. Bioanal. Chem.* **2004**, *379*, 674.
[30] C. Frausto-Reyes, M. Ortiz-Morales, J. M. Bujdud-Pérez, G. E. Magaña-Cota, R. Mejía-Falcón, *Spectrochim. Acta, Part A* **2009**, *74*, 1275.
[31] R. W. T. Wilkins, *Mineral. Mag.* **1971**, *38*, 249.
[32] R. L. Frost, *J. Raman Spectrosc.* **2004**, *35*, 153.
[33] R. J. H. Clark, T. J. Dines, *Inorg. Chem.* **1982**, *21*, 3585.
[34] W. Kiefer, H. J. Bernstein, *Mol. Phy.* **1972**, *23*, 835.
[35] E. C. Ziemath, M. A. Aegerter, F. E. A. Melo, J. E. Moreira, J. Mendes Filho, M. S. S. Dantas, M. A. Pimenta, *J. Non-Cryst. Solids* **1996**, *194*, 41.

[36] J. E. Maslar, W. S. Hurst, W. J. Bowers Jr., J. H. Hendricks, M. I. Aquino, I. Levin, *Appl. Surf. Sci.* **2001**, *180*, 102.
[37] H. C. Barshilia, K. S. Rajam, *Appl. Surf. Sci.* **2008**, *255*, 2925.
[38] M. Cherian, M. S. Rao, A. M. Hirt, I. E. Wachs, G. Deo, *J. Catal.* **2002**, *211*, 482.
[39] J. M. Alía, H. G. M. Edwards, A. Fernández, M. Prieto, *J. Raman Spectrosc.* **1999**, *30*, 105.
[40] L. Doyen, R. Frech, *J. Chem. Phys.* **1996**, *104*, 7847.
[41] D. Stoilova, M. Georgiev, D. Marinova, *J. Mol. Struct.* **2005**, *738*, 211.
[42] J. E. D. Davies, D. A. Long, *J. Chem. Soc. A* **1971**, *0*, 1275.
[43] I. M. Bell, R. J. Clark, P. J. Gibbs, *Spectrochim. Acta, Part A* **1997**, *53*, 2159.

Supporting information

Additional supporting information may be found in the online version of this article at the publisher's web site.